Journal of Statistical Physics, Vol. 35, Nos. 3/4, 1984

Behavior of the Effective Fields for a Regular Ising Model on the Cayley Tree

T. Horiguchi[1] and T. Morita[1]

Received September 15, 1983; revision received November 30, 1983

A regular Ising model with nearest-neighbor interactions of J and $-J$ ($J > 0$) on a Cayley tree of coordination number 3 is investigated for the behavior of effective fields in a uniform external field. The effective fields show periodic and also aperiodic structures in the temperature-field plane. At absolute zero temperature, the equations determining effective fields are reduced to a nonlinear, one-dimensional, iterative equation. Arithmetic furcations of period and a "screening" of the furcations are observed.

KEY WORDS: Ising model; Cayley tree; frustration; mapping; fixed points; period; arithmetic furcation; screening of furcations; spin glass; spin crystal.

1. INTRODUCTION

The Ising model on a Cayley tree is interesting not only because the system can be treated exactly but also because the thermodynamic properties of the system at the central part of the tree are the same as those of the Ising model within the Bethe approximation. The frustration effects due to competing interactions of the regular Ising model, especially the so-called ANNNI (axial next-nearest-neighbor Ising) model, give a variety of magnetic properties within the mean-field theory on regular lattices.[1-3] See also Selke and Fisher,[4] Fisher and Selke,[5] etc., for other treatments of this model. Recently investigations of an Ising model with frustration on the Cayley tree have been carried out by Vannimenus[6] and Inawashiro and Thompson[7] (see also Ref. 8). The regular Ising model with ferromag-

[1] Department of Engineering Science, Faculty of Engineering, Tohoku University, Sendai 980, Japan.

0022-4715/84/0500-0355$03.50/0

netic nearest-neighbor (NN) and antiferromagnetic next-nearest-neighbor (NNN) interactions on the Cayley tree with coordination number 3 has been studied by Vannimenus[6] in the case in which the NNN interactions between the sites on the same shell are vacant. He found the existence of a multicritical point at absolute zero temperature, where four phases such as ferromagnetic, paramagnetic, modulated, and antiferromagnetic with a $(++--)$ periodicity meet. Inawashiro and Thompson[7] and Inawashiro *et al.*[8] investigated the model in which all of the NNN interactions participate. The frustration effects in their system are much more prominent than in the system studied by Vannimenus; the modulated phase is obtained even at zero temperature.

The competition between the exchange interactions and the applied external field also produces frustration effects. Morita[9] studied a model with this type of frustration: a regular Ising model with only NN interactions of two ferromagnetic bonds and one antiferromagnetic bond in a uniform external field on a Cayley tree with coordination number 3. He gave a brief report on the model in a previous letter.[9] It was pointed out that there exist paramagnetic, spin-glass, and spin-crystal phases.

Since we want to know what happens in the system, we have investigated the structure of the effective fields. The behavior of the effective fields is quite curious, in particular at absolute zero temperature. There are two types of behavior for the period of the effective fields at zero temperature: an arithmetic furcation for small values of effective fields and a "screening" of furcations for values of effective field near and less than J. J is the magnitude of the exchange interaction. An arithmetic furcation of the period means that a periodic orbit of period $m_1 + m_2$ appears at h', a value of a parameter involved in the mapping, satisfying $h_1 < h' < h_2$, and two periodic orbits of period m_1 and m_2 exist at h_1 and h_2, respectively. "Screening" of furcations means that regions of special periodic orbits in the parameter space screen parts of the regions of other periodic orbits whose periods are obtained by arithmetic furcations. To study the arithmetic furcation, we have investigated an Ising model with l bonds with $J > 0$ and l bonds with $-J$ on a Cayley tree with coordination number $2l$, with $l \geqslant 3$ in a uniform external field at zero temperature.[10] An exact analysis has been given for a one-dimensional mapping obtained from the iterative equations for the effective fields of the Ising model on the Cayley tree.[11]

In the present paper, we report our detailed investigations of the system studied by Morita,[9] by focusing on the structure of the effective fields which satisfy nonlinear coupled iterative equations. We obtain a phase boundary between a phase with a shorter periodic orbit and a phase with a longer periodic orbit or an aperiodic orbit. We calculate correlation

functions of effective fields as a function of the shell number. The wave number associated with the shell number is calculated from the correlation functions. From the analyses, it turns out that the spin-crystal phase corresponds to commensurate phase with shell number and the spin-glass phase to the incommensurate phase. At zero temperature, the equations for the effective fields are reduced to a one-dimensional, piecewise linear, iterative equation. It is found by numerical calculations that the arithmetic furcations of period occur as a function of h for $h \leqslant 2J/3$, where h is the external field, and that the dominant periods 14 and 7 screen some periods from arithmetic furcations for $2J/3 \leqslant h < J$.

In Section 2, we describe the Ising model on a Cayley tree and investigate a set of nonlinear equations for effective fields at finite temperature. In Section 3, it is reduced to a set of piecewise linear iterative equations at absolute zero temperature. We find a projection of the two-dimensional mapping to a one-dimensional mapping and give detailed discussions on that one-dimensional mapping. Concluding remarks are given in Section 4. In Appendix A, we define a sequence of positive integers which is a representation of the periods when their furcation is arithmetic. In Appendix B, we give expressions of the regions on which the one-dimensional mappings are defined.

2. ISING MODEL ON A CAYLEY TREE

We consider the Cayley tree which has a central site 0 and N shells surrounding it. The coordination number of the tree is assumed to be 3. We label the shells in order from the outermost to the innermost, then the central site is on the Nth shell. The sites except those on the 0th shell (the 0th shell is referred to as the surface of the Cayley tree) have three nearest-neighbor sites and those on the surface have only one nearest-neighbor site. There is an Ising spin on each site. Each spin except on the surface interacts with two nearest-neighbor spins by $J > 0$ and one nearest-neighbor spin by $-J$. The spin directions are uniquely determined if the direction of the spin at the central site is up and there is no external field; there is frustration when the uniform external field is applied.

We introduce two types of effective fields $h_s^{(+)}$ and $h_s^{(-)}$ to a site on the sth shell from the outermost branch, depending upon whether the interaction between the site and its nearest-neighbor site on the $(s-1)$th shell is J or $-J$. The effective fields $h_s^{(\pm)}$ are determined as follows:

$$\exp(2\beta h_s^{(+)}) = Z_s^{+-}(+)/Z_s^{+-}(-)$$

$$\exp(2\beta h_s^{(-)}) = Z_s^{++}(+)/Z_s^{++}(-)$$

where

$$Z_s^{++}(\sigma) = \sum_{\sigma'} \exp\left[\beta\sigma'\left(h + 2h_{s-1}^{(+)}\right) - \beta J\sigma\sigma'\right]$$

$$Z_s^{+-}(\sigma) = \sum_{\sigma'} \exp\left[\beta\sigma'\left(h + h_{s-1}^{(+)} + h_{s-1}^{(-)}\right) + \beta J\sigma\sigma'\right]$$

h is the uniform external field and $\beta = 1/kT$ as usual. $h_{(s-1)}^{(\pm)}$ are the effective fields on a site on the $(s-1)$th shell from the outermost branch. The iterative equations determining the effective fields are given by

$$\begin{aligned} h_s^{(+)} &= \beta^{-1}\tanh^{-1}\left[\tanh(\beta J)\tanh\beta\left(h + h_{s-1}^{(+)} + h_{s-1}^{(-)}\right)\right] \\ h_s^{(-)} &= -\beta^{-1}\tanh^{-1}\left[\tanh(\beta J)\tanh\beta\left(h + 2h_{s-1}^{(+)}\right)\right] \end{aligned} \tag{2.1}$$

At the surface, i.e., $s = 0$, we assume $h_0^{(\pm)} = 0$. This set of equations is a set of nonlinear, coupled, iterative equations. We are interested in the behavior of effective fields in the limit of $N \to \infty$.

In order to investigate the mapping (2.1), we introduce new variables $x_s = \tanh \beta h_s^{(+)}$, $y_s = \tanh \beta h_s^{(-)}$, $a = \tanh \beta J$ and $b = \tanh \beta h$. Then we have

$$x_s = a(b + x_{s-1} + y_{s-1} + bx_{s-1}y_{s-1})/(1 + bx_{s-1} + by_{s-1} + x_{s-1}y_{s-1}) \tag{2.2}$$

$$y_s = -a\left(b + 2x_{s-1} + bx_{s-1}^2\right)/\left(1 + 2bx_{s-1} + x_{s-1}^2\right)$$

where $x_0 = y_0 = 0$. Equations (2.2) are expressed as follows:

$$(x_s, y_s) = \Psi(x_{s-1}, y_{s-1}) = \Psi^k(x_{s-k}, y_{s-k}) \tag{2.3}$$

An orbit is given by $\Omega \equiv \{(x_s, y_s)\}_{s=0,1,2,\ldots}$. The orbit is periodic if it is finite. The period is defined by the least integral p such that there exists an integral M and for any integral $i \geqslant M$, $(x_{i+p}, y_{i+p}) = (x_i, y_i)$.

There is only one fixed point (x_∞, y_∞) of the mapping (2.3). x_∞ is determined as the positive root of the equation:

$$\begin{aligned} &b(1-a)x^4 + (1 - 3a + 2b^2 - ab^2 + a^2b^2)x^3 + 3b(1-a)^2x^2 \\ &\quad + (1 - a - 3ab^2 + 2a^2 + a^2b^2)x - ab(1-a) = 0 \end{aligned} \tag{2.4}$$

y_∞ is given by

$$y_\infty = -a\left(b + 2x_\infty + bx_\infty^2\right)/\left(1 + 2bx_\infty + x_\infty^2\right) \tag{2.5}$$

These equations (2.4) and (2.5) are equivalent to those obtained by Morita.[9] By expanding x_s and y_s around the fixed points, we find the region where the fixed point is stable. The region is determined by the

following condition:

$$2d_+ d_- < 1$$

where

$$d_+ = a(1 - x_\infty^2)(1 - b^2)/(1 + bx_\infty + by_\infty + x_\infty y_\infty)^2$$

$$d_- = a(1 - x_\infty^2)(1 - b^2)/(1 + 2bx_\infty + x_\infty^2)^2$$

This region is the hatched one with number 1 in Fig. 1. The spin state in this region corresponds to the paramagnetic state. When $h = 0$, $x_\infty = y_\infty = 0$, and $d_+ = d_- = \tanh \beta J$. The critical temperature T_c between the paramagnetic phase and the other phase is given by

$$J/kT_c = \tanh^{-1}(1/\sqrt{2})$$

We obtained numerically the values of effective fields from the set of equations (2.2). At low temperatures, Eq. (2.2) are not suitable for numerical calculations. Then we use the following expansions obtained from Eq.

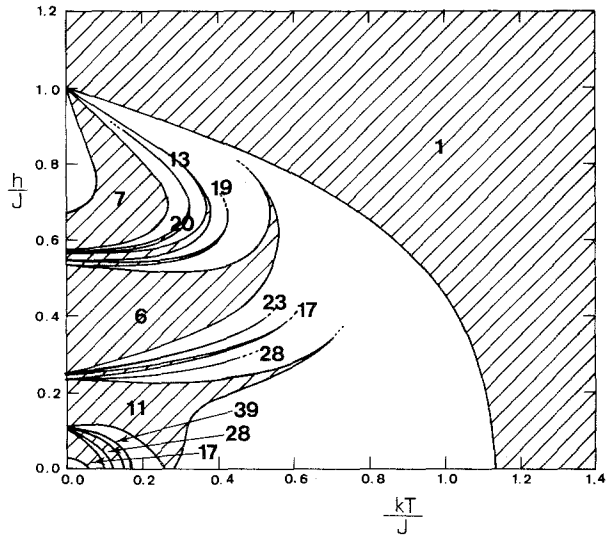

Fig. 1. The phase diagram in the temperature-field plane is shown. We have periodic orbits in the hatched regions. The number attached to the region shows the period of orbits. We have longer periodic or aperiodic orbits in the regions not hatched.

(2.1):

$$h_s^{(+)} = \frac{1}{2}\{|J + h + h_{s-1}^{(+)} + h_{s-1}^{(-)}| - |J - h - h_{s-1}^{(+)} - h_{s-1}^{(-)}|\}$$
$$+ \frac{1}{2\beta}\sum_{n=1}^{\infty}\frac{(-1)^{n-1}}{n!}\left[\exp(-2\beta n|J + h + h_{s-1}^{(+)} + h_{s-1}^{(-)}|)\right.$$
$$\left. - \exp(-2\beta n|J - h - h_{s-1}^{(+)} - h_{s-1}^{(-)}|)\right]$$

$$h_s^{(-)} = -\frac{1}{2}\{|J + h + 2h_{s-1}^{(+)}| - |J - h - 2h_{s-1}^{(+)}|\}$$
$$+ \frac{1}{2\beta}\sum_{n=1}^{\infty}\frac{(-1)^{n}}{n!}\left[\exp(-2\beta n|J + h + 2h_{s-1}^{(+)}|)\right.$$
$$\left. - \exp(-2\beta n|J - h - h_{s-1}^{(+)}|)\right]$$

We found periodic orbits in some regions in the T–h plane. Some of them are shown in Fig. 1 by the hatched regions. For an aperiodic orbit, we have an attractor which seems to be a continuous closed curve. For a periodic orbit, it collapses to a discrete set of points. In the numerical calculations, we cannot discriminate between a longer periodic orbit and an aperiodic orbit. In order to find boundaries in the $T - h$ plane at which an aperiodic orbit turns to a periodic orbit, we calculated the Lyapunov exponent defined by Vannimenus[6] and obtained a negative exponent for a periodic orbit and zero for an aperiodic orbit. However, we failed to find the

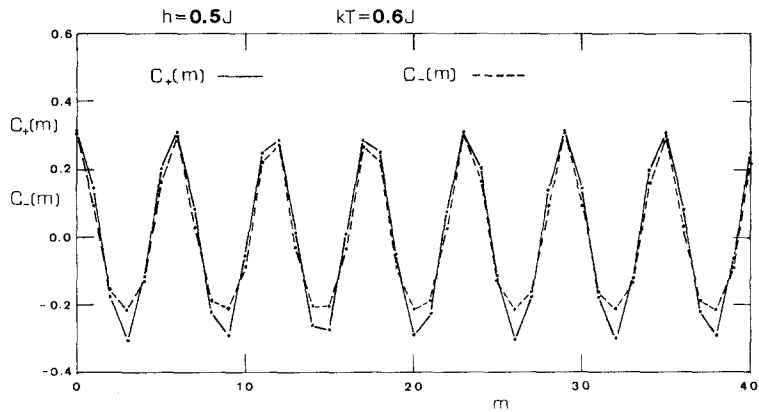

Fig. 2. The autocorrelation functions of x_s and y_s are shown as a function of shell number m for $kT/J = 0.6$ and $h/J = 0.5$.

boundaries. It turned out by further calculations for values of effective fields with more decimal places for T and h that the regions for periodic orbits intervene between those for an aperiodic orbit in whisker shapes and vice versa, as partly seen in Fig. 1. We did not show there the regions for longer periodic orbits. Then in the regions which are not hatched, there exist longer periodic or aperiodic orbits.

In a prevous letter,[9] a spin state determined by a periodic orbit is called a spin-crystal state and that by an aperiodic orbit the spin-glass state. In order to see the behavior of effective fields in the region of longer periodic or aperiodic orbits, we define autocorrelation functions of x_s and y_s as follows:

$$C_+(m) = \lim_{N\to\infty} \frac{1}{N} \sum_{j=1}^{N} (x_{m+j} - \bar{x})(x_j - \bar{x})$$

$$C_-(m) = \lim_{N\to\infty} \frac{1}{N} \sum_{j=1}^{N} (y_{m+j} - \bar{y})(y_j - \bar{y})$$

where

$$\bar{x} = \lim_{N\to\infty} \frac{1}{N} \sum_{s=1}^{N} x_s$$

$$\bar{y} = \lim_{N\to\infty} \frac{1}{N} \sum_{s=1}^{N} y_s$$

The behavior of $C_-(m)$ as a function of m is much the same as the one of

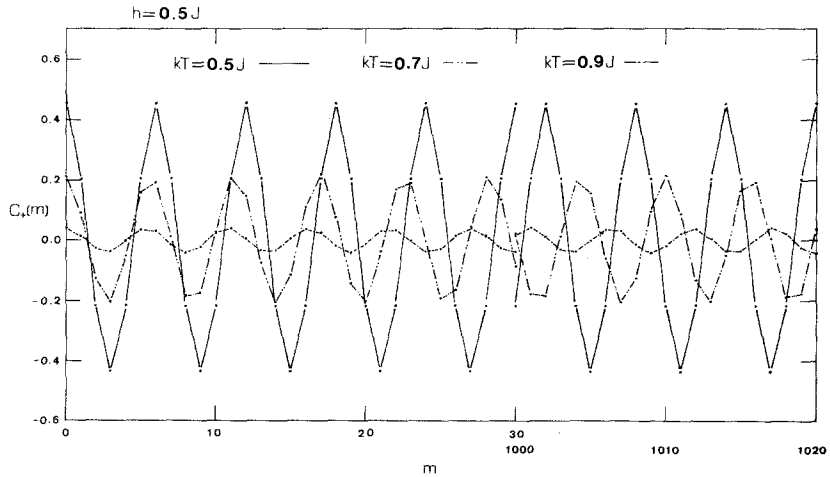

Fig. 3. The autocorrelation function of x_s is shown as a function of shell number for values of temperature $kT/J = 0.5$, 0.7, and 0.9 at a fixed external field $h/J = 0.5$.

$C_+(m)$. For example, see Fig. 2, where we show the behavior of $C_+(m)$ and $C_-(m)$ for $h/J = 0.5$ and $kT/J = 0.6$. Thus we consider only $C_+(m)$ hereafter. In Fig. 3, we show $C_+(m)$ and $C_+(m + 1000)$ for $kT/J = 0.5$, 0.7, and 0.9 and for $h/J = 0.5$. We see from Fig. 1 that $C_+(m)$ is periodic for $kT/J = 0.5$ and $h/J = 0.5$. We believe that the amplitude of $C_+(m)$ does not decay as a function of m even for aperiodic cases, although whether an orbit is periodic with long period or aperiodic is hard to determine by numerical calculations. In Fig. 4, we show $C_+(m)$ for $h/J = 0.1$, 0.4, and 0.7, and for $kT/J = 0.5$. $C_+(m)$ is aperiodic but seems to be almost periodic. In case where $C_+(m)$ changes its sign as a function of m, we regard the quantity defined by the following equation as the wave number:

$$q = \lim_{N\to\infty} \frac{1}{2N} \sum_{m=1}^{N} \theta(-C_+(m)C_+(m+1))$$

where $\theta(x) = 1$ for $x > 0$, $1/2$ for $x = 0$, and 0 for $x < 0$. We set $q = 1$ when the fixed point is stable. In Fig. 5, we show q^{-1} as a function of temperature for $h/J = 0.2$, 0.4, 0.6, and 0.8. In the regions of periodic orbits, the effective fields are commensurate with shell number and in the regions of aperiodic orbits, the effective fields are incommensurate. In Fig. 6, we show q^{-1} as a function of external field for $kT/J = 0$, 0.2, 0.4, 0.6, and 0.8. Regions of h where the effective fields are commensurate are

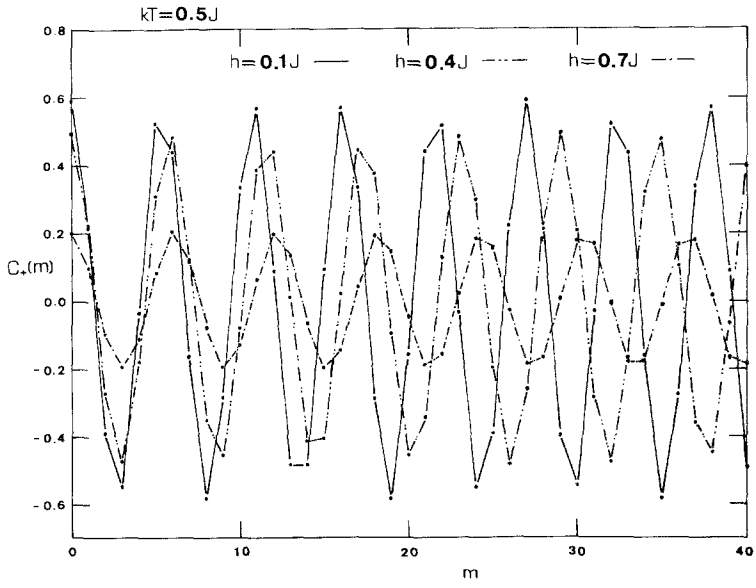

Fig. 4. The autocorrelation function of x_s is shown as a function of shell number for values of external field $h/J = 0.1$, 0, 4 and 0.7 at a fixed temperature $kT/J = 0.5$.

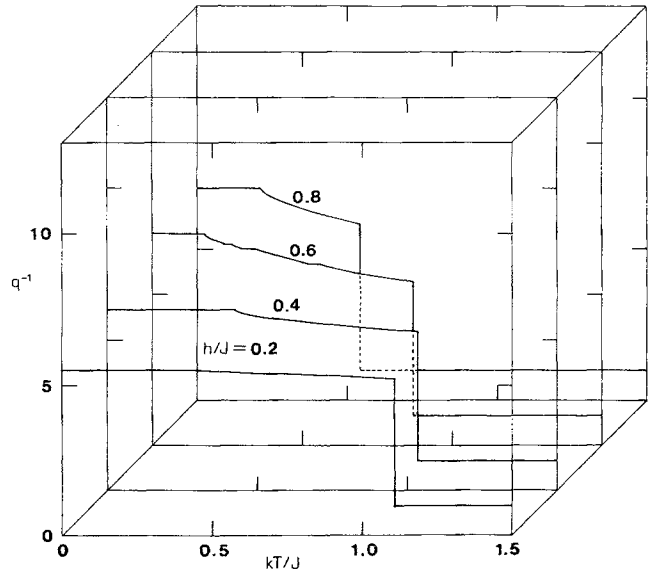

Fig. 5. The inverse of the wave number is shown as a function of temperature for values of external field $h/J = 0.2$, 0.4, 0.6, and 0.8.

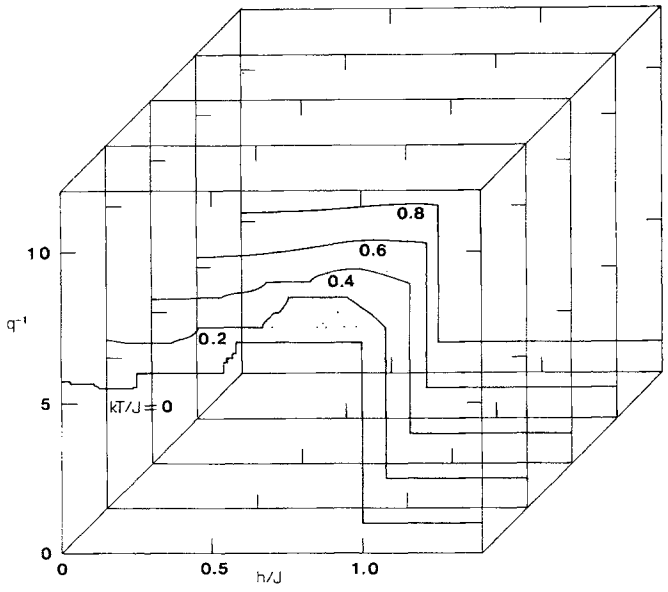

Fig. 6. The inverse of the wave number is shown as a function of the external field for values of temperature $kT/J = 0.0$, 0.2, 0.4, 0.6, and 0.8.

dominant at low temperatures, but those where the effective fields are incommensurate are dominant at high temperatures. This is due to the competition between the ordering energy and the thermal agitation. At $T = 0$ in Fig. 6, q^{-1} has several jumping points for $q^{-1} > 7$. We will discuss the case of $T = 0$ in the next section.

3. EFFECTIVE FIELDS AT $T = 0$

In the present section we investigate the behavior of effective fields at absolute zero temperature. At $T = 0$, equations (2.1) are reduced to the following ones:

$$\begin{aligned} h_s^{(+)} &= \tfrac{1}{2}\{|J + h + h_{s-1}^{(+)} + h_{s-1}^{(-)}| - |J - h - h_{s-1}^{(+)} - h_{s-1}^{(-)}|\} \\ h_s^{(-)} &= -\tfrac{1}{2}\{|J + h + 2h_{s-1}^{(+)}| - |J - h - 2h_{s-1}^{(-)}|\} \end{aligned} \tag{3.1}$$

with $h_0^{(\pm)} = 0$. We performed numerical calculations of this set of iterative equations for $h < J$. The period of orbit $\{(h_s^{(+)}, h_s^{(-)})\}_{s=0,1,2,\ldots}$ with $h_0^{(\pm)} = 0$ is given in Table I. The critical values of h at which the period

Table I. The Critical Values of h at which the Period Changes Listed up to the Fourth Decimal Place

h/J	Width	p	q^{-1}
0.0244—0.1001	0.0757	17	5.667
0.1001—0.1004	0.0003	45	5.625
0.1004—0.1098	0.0094	28	5.6
0.1098—0.1110	0.0012	39	5.571
0.1110—0.1111	0.0001	50	5.556
0.1111—0.1112	0.0001	61	5.545
0.1112—0.2308	0.1196	11	5.5
0.2308—0.2309	0.0001	50	5.556
0.2309—0.2311	0.0002	39	5.571
0.2311—0.2333	0.0022	28	5.6
0.2333—0.2334	0.0001	45	5.625
0.2334—0.2478	0.0144	17	5.667
0.2478—0.2497	0.0019	23	5.75
0.2497—0.2500	0.0003	29	5.8
0.2500—0.5385	0.2885	6	6
0.5385—0.5386	0.0001	31	6.2
0.5386—0.5393	0.0007	25	6.25
0.5393—0.5434	0.0041	19	6.333
0.5434—0.5435	0.0001	32	6.4
0.5435—0.5671	0.0236	13	6.5
0.5671—0.5672	0.0001	33	6.6
0.5672—0.5708	0.0036	20	6.667
0.5708—0.5714	0.0006	27	6.75
0.5714—0.5715	0.0001	34	6.8
0.5715—0.6667	0.0952	7	7

Table I. (Continued)

h/J	Width	p	q^{-1}
0.6667—0.6875	0.0208	14	7
0.6875—0.6876	0.0001	7	7
0.6876—0.6925	0.0049	14	7
0.6925—0.6927	0.0002	29	7.25
0.6927—0.6931	0.0004	14	7
0.6931—0.6942	0.0011	22	7.333
0.6942—0.6961	0.0019	14	7
0.6961—0.6962	0.0001	37	7.4
0.6962—0.6963	0.0001	14	7
0.6963—0.7001	0.0038	15	7.5
0.7001—0.7008	0.0007	30	7.5
0.7008—0.7012	0.0004	14	7
0.7012—0.7013	0.0001	67	7.444
0.7013—0.7014	0.0001	37	7.4
0.7014—0.7102	0.0088	14	7
0.7102—0.7103	0.0001	67	7.444
0.7103—0.7110	0.0007	14	7
0.7110—0.7112	0.0002	23	7.667
0.7112—0.7135	0.0023	14	7
0.7135—0.7136	0.0001	38	7.6
0.7136—0.7500	0.0364	14	7
0.7500—0.7501	0.0001	7	7
0.7501—0.8000	0.0499	14	7
0.8000—0.8001	0.0001	7	7
0.8001—0.8125	0.0124	14	7
0.8125—0.8126	0.0001	15	7.5
0.8126—0.8400	0.0274	14	7
0.8400—0.8401	0.0001	7	7
0.8401—0.8425	0.0024	14	7
0.8425—0.8426	0.0001	29	7.25
0.8426—0.8450	0.0024	14	7
0.8450—0.8451	0.0001	22	7.333
0.8451—0.8500	0.0049	14	7
0.8500—0.8501	0.0001	15	7.5
0.8501—0.8700	0.0199	14	7
0.8700—0.8701	0.0001	23	7.667
0.8701—0.8750	0.0049	14	7
0.8750—0.8751	0.0001	7	7
0.8751—0.8800	0.0049	14	7
0.8800—0.8801	0.0001	15	7.5
0.8801—0.9000	0.0199	14	7
0.9000—0.9001	0.0001	7	7
0.9001—0.9200	0.0199	14	7
0.9200—0.9201	0.0001	8	8
0.9201—0.9250	0.0049	14	7
0.9250—0.9251	0.0001	15	7.5
0.9251—0.9375	0.0124	14	7
0.9375—0.9376	0.0001	7	7
0.9376—0.9400	0.0024	14	7
0.9400—0.9401	0.0001	15	7.5
0.9401—0.9500	0.0099	14	7

changes are listed up to the fourth decimal place in Table I for h between $0.0244J$ and $0.95J$. We express in Table I that the period p_1 appears at each value of h such that $h_1, h_1 + \Delta h, \ldots, h_2 - \Delta h$ when the row is $h_1 - h_2, \Delta h$, p_1, q_1^{-1}. We see that the behavior of the period as a function of h changes at $0.6667J$. For $h < 0.6667J$, it seems that we have arithmetic furcations of period. Here the arithmetic furcation of the period means that a periodic orbit of period $m_1 + m_2$ appears at value of h' satisfying $h_1 < h' < h_2$ where h_1 and h_2 are fields for which orbits of period m_1 and m_2, respectively, are stable. For $h < 0.0239J$, although we do not give the results in Table I, we seem to have $P(6m + 11, 6m + 17)$ with $m = 1, 2, \ldots$. See Appendix A for the definition of a sequence $P(m, m')$. For $h \geqslant 0.75J$, we found a regularity in the results; a set of periods for $0.75J \leqslant h < 0.95J$ appears repeatedly in the following ranges with $N = 1, 2, \ldots$:

$$0.75 + \sum_{n=1}^{N} 0.2^n \leqslant h/J < 0.75 + \sum_{n=1}^{N+1} 0.2^n$$

We therefore do not place the results for $h \geqslant 0.95J$ in Table I.

We denote equations (3.1) as follows:

$$\left(h_s^{(+)}, h_s^{(-)}\right) = \Phi\left(h_{s-1}^{(+)}, h_{s-1}^{(-)}\right) = \Phi^k\left(h_{s-k}^{(+)}, h_{s-k}^{(-)}\right)$$

where Φ is a continuous and piecewise linear mapping. When $h < J$, we have an unstable fixed point $(0, -h)$. When $h = J$, we have a line of stable fixed points expressed by the set $\{(x, y) \mid 0 < x \leqslant J,\ y = -J\}$. When $h > J$, we have a stable fixed point $(J, -J)$. Thus we investigate in detail only the case of $h < J$.

We define the following regions E, E_5, and K:

$$E = \{(x, y) \mid |x + y + h| < J, |2x + h| < J\}$$

$$E_5 = \{(x, y) \mid (x, y) \in E, |y + h - x| < J, |x + y + 3h/2| < J/2\}$$

$$K = \{(x, y) \mid |x| \leqslant J, y = -J\}$$

Every point (x, y) in $R^2 - E_5$ is mapped into the region K within five operations of the mapping. Every point of E_5 is mapped into E and then possibly to a point in E_5 itself. When points $(h_{s+j}^{(+)}, h_{s+j}^{(-)})$ are in E_5 for $j = 0, 1, 2, \ldots, l - 1$, then $h_{s+j}^{(\pm)}$ for $j = 1, 2, \ldots, l$ take the following forms:

$$h_{s+l}^{(+)} = a_{l+2} h_s^{(+)} + a_{l+1}\left(h_s^{(-)} + h\right)$$

$$h_{s+l}^{(-)} = -2a_{l+1} h_s^{(+)} - 2a_l\left(h_s^{(-)} + h\right) - h$$

Here a_l are determined by the recurrence equation:

$$a_{l+2} = a_{l+1} - 2a_l$$

with $a_1 = 0$ and $a_2 = 1$. a_l is expressed as follows:

$$a_l = \frac{1}{\sqrt{7}} 2^{(1/2)(l+1)} \sin(l-1)\theta$$

where

$$\theta = \sin^{-1} \frac{\sqrt{7}}{2\sqrt{2}}$$

Then the point $(h_{s+l}^{(+)}, h_{s+l}^{(-)})$ satisfies the relation:

$$2h_{s+l}^{(+)^2} + h_{s+l}^{(+)}\left(h_{s+l}^{(-)} + h\right) + \left(h_{s+l}^{(-)} + h\right)^2$$
$$= 2^l \left\{ 2h_s^{(+)^2} + h_s^{(+)}\left(h_s^{(-)} + h\right) + \left(h_s^{(-)} + h\right)^2 \right\}$$

Thus there exists for each point $(h_s^{(+)}, h_s^{(-)})$ in E_5 a number $\tilde{N}$ such that

$$\tilde{N} = \left[\log_2 \frac{2h^2 + 5hJ + 4J^2}{2h_s^{(+)^2} + h_s^{(+)}\left(h_s^{(-)} + h\right) + \left(h_s^{(-)} + h\right)^2} \right] - 1$$

and the point $(h_{s+j}^{(+)}, h_{s+j}^{(-)})$ for $j > \tilde{N}$ should already be outside of E_5. In this way, every point in R^2 except the unstable fixed point $(0, -h)$ is mapped to the set K.

We consider a projection of the two-dimensional mapping Φ to a one-dimensional mapping φ_k defined by

$$h_{s+k}^{(+)} = \varphi_k\left(h_s^{(+)}\right) \tag{3.2}$$

Here Eq. (3.2) denotes the following equation:

$$\left(h_{s+k}^{(+)}, h_{s+k}^{(-)} = -J\right) = \Phi^k\left(h_s^{(+)}, h_s^{(-)} = -J\right)$$

where we assume that $h_{s+j}^{(-)} \neq -J$ for $1 \leqslant j < k$. In Eq. (3.2), the subscript k of φ_k is also a function of $h_s^{(+)}$. The periodic orbit of $h_s^{(+)}$ determined by (3.2) is $\{h_s^{(+)}, h_{s+k_1}^{(+)}, h_{s+k_1+k_2}^{(+)}, \ldots\}$. Obtaining the φ_k is elementary but tedious. We give only the results. We consider 15 regions $R_1, R_2, \ldots, R_{15}$ in the $h - x$ plane which are shown in Fig. 7; their expressions are given in Appendix B. φ_k is given on these regions as follows:

$$\varphi_1 = x - J + h \text{ in } R_1, \qquad \varphi_5 = J \text{ in } R_2, \qquad \varphi_5 = 4x - J + 4h \text{ in } R_3$$
$$\varphi_5 = J - 2h \text{ in } R_4, \qquad \varphi_5 = 6x - J + 2h \text{ in } R_5, \qquad \varphi_5 = 5x + J - h \text{ in } R_6$$
$$\varphi_5 = 2x + J - 4h \text{ in } R_7, \qquad \varphi_4 = 4x + J - 2h \text{ in } R_8, \qquad \varphi_4 = J \text{ in } R_9$$
$$\varphi_4 = -x + 3J - 3h \text{ in } R_{10}, \qquad \varphi_4 = 2x + 3J - 2h \text{ in } R_{11},$$
$$\varphi_4 = 4x + 3J \text{ in } R_{12} \qquad \varphi_4 = J - 2h \text{ in } R_{13}, \qquad \varphi_3 = J \text{ in } R_{14}$$

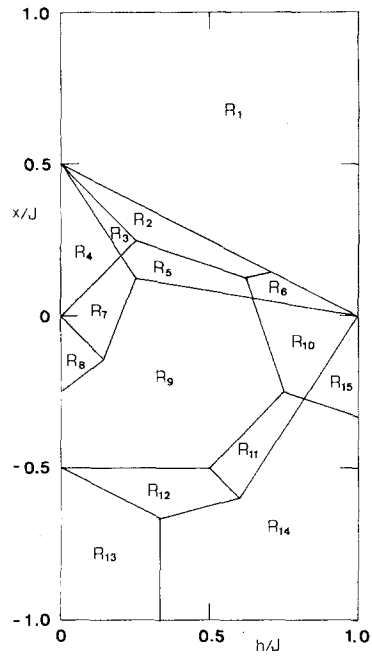

Fig. 7. The regions in the h–x plane are shown. At each region, we have a different, one-dimensional mapping φ_k.

and

$$\varphi_3 = -3x + J - h \text{ in } R_{15}$$

The function φ_k is piecewise linear for $-J \leqslant x \leqslant J$ at a fixed h.

φ_k is shown by solid lines in Figs. 8a–l for $h = 0.1J$, $0.11J$, $0.2J$, $0.24J$, $0.3J$, $0.4j$, $0.5J$, $0.6J$, $0.7J$, $0.8J$, $0.9J$, and $0.91J$, respectively. The processes of the mapping are shown by the broken lines. Suppose that a broken line starting from a point belonging to the set of periodic points visits φ_k ν_k times before it comes back to the starting point; then the period is given by

$$p = \nu_1 + 4\nu_4 + 5\nu_5$$

For example, we have period 39 and 11 in Figs. 8b and 8c, respectively, and period 7 and 14 in Figs. 8k and 8l, respectively.

First we consider the cases of $0 < h \leqslant 7J/13$. In Figs. 8c, 8d, and 8e, we show how an orbit of period 17 is obtained between the orbits of period 11 and 6. We notice that there are several types of periodic orbit with the

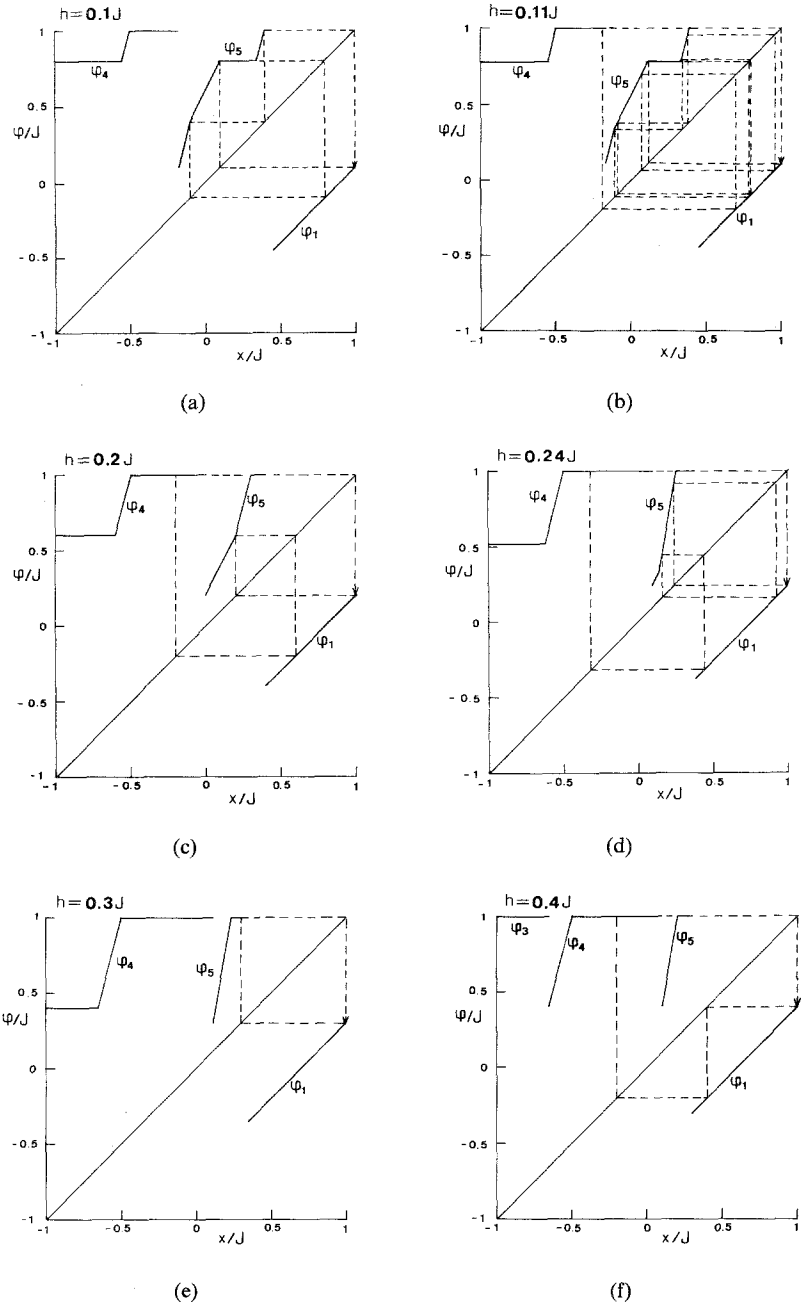

Fig. 8. The one-dimensional mapping φ_k and the processes of the mapping are shown in from (a) to (l) for $h/J = 0.1$, 0.11, 0.2, 0.24, 0.3, 0.4, 0.5, 0.6, 0.7, 0.8, 0.9, and 0.91, respectively.

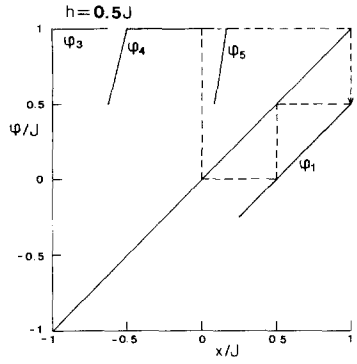

(g)

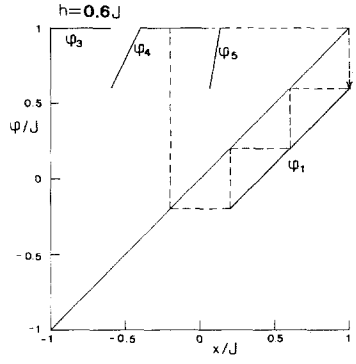

(h)

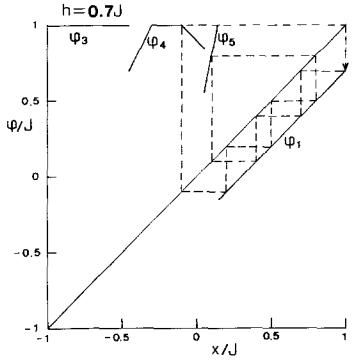

(i)

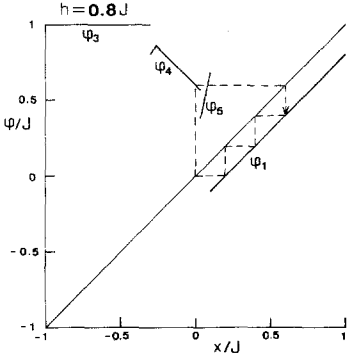

(j)

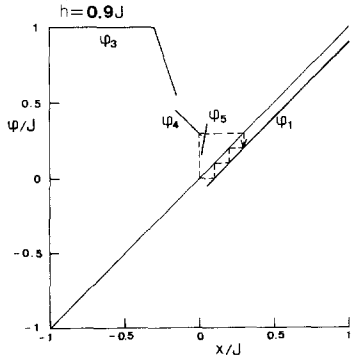

(k)

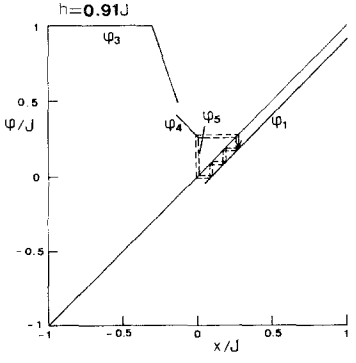

(l)

Fig. 8. (Continued)

same period. For example, there are three types of periodic orbit of period 11: $\{J, h, -J+8h, -2J+9h\}$, $\{J, h, J-2h, -h\}$, and $\{J-2h, -h, J-6h, -5h\}$. Since the number of times of visiting the dangler of φ_5 changes with the values of h, we obtain a sequence of periods $P(11,6)$ for $J/9 \leqslant h \leqslant 7J/13$. Similarly, we obtain a sequence of periods $P(17,11)$ for $J/41 \leqslant h \leqslant 3J/13$, a sequence of periods $P(23,17)$ for $J/169 \leqslant h \leqslant J/10$ and so on. As an example, we show in Fig. 8b an orbit of period 39 which is obtained between the orbits of period 28 and 11; the orbit of period 28 is obtained between the orbits of period 17 and 11 in Figs. 8a and 8c, respectively. We have the following relations from Eq. (A1):

$$\begin{aligned} P(11,6) &= P(11,17) + P(17,6) \\ &= P(11,17) + P(17,23) + P(23,6) \\ &= \lim_{N\to\infty} \left\{ \sum_{j=1}^{N} P(11+6(j-1), 11+6j) + P(11+6N, 6) \right\} \end{aligned}$$

This relation is confirmed in Table I in the range of h: $0.1112J \leqslant h < 0.5385J$. Second, we consider the case of $J/4 \leqslant h \leqslant 2J/3$. As seen from Figs. 8e–h, φ_1 in R_1, φ_5 in R_2, φ_5 in R_5, and φ_4 in R_9 determine the orbits. Since the number of times of visiting the dangler of φ_5 changes with the value of h, we obtain a sequence of periods $P(6,7)$ for $J/4 \leqslant h \leqslant 2J/3$. Lastly, we consider the case of $2J/3 \leqslant h < J$. As shown in Figs. 8i–l we encounter a new situation. We have the φ_4 in R_{10}, which is a line with slope -1. As the external field increases, only this part survives for φ_4. This φ_4 stabilizes orbits with periods 14 and 7. Thus the arithmetic furcation due to the φ_5 in R_6 is "screened" by the φ_4 in R_{10}. We call this phenomenon a "screening" of the furcations. This is seen for $2J/3 \leqslant h < J$.

The inverse of the wave number, q^{-1}, defined in Section 2 is expressed as follows:

$$q^{-1} = p/(\nu_4 + \nu_5)$$

q^{-1} is also given in Table I. The generation of several jumping points at $T = 0$ in Fig. 6 mentioned in Section 2 is now understood.

4. CONCLUDING REMARKS

In the present paper, we have investigated the behavior of effective fields for the regular Ising model with nearest-neighbor interactions of $J > 0$ and $-J$ on the Cayley tree of coordination number 3 under the uniform external field. The frustration effects between the exchange interactions and the uniform external field produce curious behaviors of the

effective fields; the effective fields have periodic and aperiodic structures as a function of shell number. At $T = 0$, only periodic structures appear. The period of the effective fields furcates as a function of the external field. There are the arithmetic furcations and the "screening" of the furcations in the present systems. The arithmetic furcation is popular in physical systems with frustration (see, for example, Aubry,[12] Bak,[13] and Aubry[14]).

It is confirmed by numerical calculations that the screening of the furcations also occurs at finite temperature, more precisely at the low-temperature region surrounded by that of period 7 in Fig. 1. We believe that the screening of the furcations is a new type. It would be much more interesting if the screening of the furcations occurs in more realistic systems. As mentioned by Morita,[9] the system studied in the present paper is regarded as a model for the Ising model on the honeycomb lattice in which each ferromagnetic hexagon is connected to the surrounding six ferromagnetic hexagons by antiferromagnetic bonds. Here the ferromagnetic hexagon means that each bond in the hexagon is ferromagnetic. It is expected that the screening of the furcations occurs in that Ising model on the honeycomb lattice. Investigations of such system are left to future works.

APPENDIX A

We define sequences of positive integers related to two different positive integers, m and m', in this appendix.

Consider a sequence $\{m, m'\}$ and denote it by $P_0(m, m')$. Let us call m and m' a successive pair in $P_0(m, m')$. We insert $m + m'$ between m and m' and obtain a new sequence $\{m, m + m', m'\}$. We denote it by $P_1(m, m')$. Let us call m and $m + m'$, and also $m + m'$ and m' successive pairs in $P_1(m, m')$. For every successive pair m_1 and m_2 in sequences $P_n(m, m')$, we calculate $m_1 + m_2$ and insert it between m_1 and m_2. Then we obtain a new sequence $P_{n+1}(m, m')$. Let us call m_1 and $m_1 + m_2$, and also $m_1 + m_2$ and m_2, for each successive pair m_1 and m_2 in $P_n(m, m')$, successive pairs in $P_{n+1}(m, m')$. In this way, we can define sequences $P_0(m, m'), P_1(m, m'), P_2(m, m'), \ldots,$ inductively. Finally, we define an infinite sequence of positive integers by

$$P(m, m') = \lim_{n \to \infty} P_n(m, m')$$

We define an addition of two sequences $P_n(m, m + m')$ and $P_n(m + m', m')$ by

$$P_n(m, m') = P_n(m, m + m') + P_n(m + m', m')$$

Then we have the following relation:

$$P(m,m') = P(m,m+m') + P(m+m',m') \tag{A1}$$

We look into the structure of the sequence $P(m,m')$, then we find infinitely many arithmetic progressions in $P(m,m')$. When the period of the oribit in a mapping takes on all the numbers in the sequence $P(m,m')$ as a function of parameter involved in the mapping, we say that an arithmetic furcation of period takes place between m and m' as a function of the parameter.

APPENDIX B

We give the expressions of 15 regions, which are shown in Fig. 7, in the following:

$$R_1 = \{0 < h < J, (J-h)/2 \leqslant x \leqslant J\}$$

$$R_2 = \{x \leqslant (J-h)/2, x \geqslant J/2 - h, x \geqslant (J-h)/3, x \geqslant h/5\}$$

$$R_3 = \{x \leqslant J/2 - h, x \geqslant (J-3h)/2, x \geqslant h\}$$

$$R_4 = \{h > 0, x \leqslant (J-3h)/2, x \geqslant h\}$$

$$R_5 = \{x \leqslant h, x \leqslant (J-h)/3, x \leqslant 2J-3h, x \geqslant (J-3h)/2, x \geqslant (J-h)/6\}$$

$$R_6 = \{x \leqslant h/5, x \leqslant (J-h)/2, x \geqslant 2J-3h, x \geqslant (J-h)/6\}$$

$$R_7 = \{x \leqslant h, x \leqslant (J-3h)/2, x \geqslant -h, x \geqslant (-J+5h)/2\}$$

$$R_8 = \{h > 0, x \leqslant -h, x \geqslant (-J+3h)/4\}$$

$$\begin{aligned} R_9 = {} & \{0 < h \leqslant J/7, x \leqslant (-J+3h)/4, x \geqslant -J/2\} \\ & + \{x \leqslant (-J+5h)/2, x \leqslant (J-h)/6, \\ & \quad x \leqslant 2J-3h, x \geqslant -J/2, x \geqslant -J+h\} \end{aligned}$$

$$R_{10} = \{x \leqslant (J-h)/6, x \geqslant 2J-3h, x \geqslant -h/3, x \geqslant 3(-J+h)/2\}$$

$$R_{11} = \{x \leqslant -J+h, x \leqslant -h/3, x \geqslant -h, x \geqslant 3(-J+h)/2\}$$

$$R_{12} = \{x \leqslant -J/2, x \leqslant -h, x \geqslant -(J+h)/2, x \geqslant (-3J+h)/4\}$$

$$R_{13} = \{0 < h \leqslant J/3, -J \leqslant x \leqslant -(J+h)/2\}$$

$$\begin{aligned} R_{14} = {} & \{J/3 \leqslant h \leqslant 3J/5, -J \leqslant x \leqslant (-3J+h)/4\} \\ & + \{3J/5 \leqslant h < J, x \leqslant 3(-J+h)/2, x \leqslant -h/3, x \geqslant -J\} \end{aligned}$$

$$R_{15} = \{h < J, x \leqslant 3(-J+h)/2, x \geqslant -h/3\}$$

REFERENCES

1. P. Bak and J. von Boehm, *Phys. Rev. B* **21**:5297 (1980).
2. P. Bak, *Phys. Rev. Lett.* **46**:791 (1981).
3. C. S. O. Yokoi, M, D. Contiho-Filho, and R. S. Salinas, *Phys. Rev. B* **24**:4047 (1981).
4. W. Selke and M. E. Fisher, *Phys. Rev. B* **20**:257 (1979).
5. M. E. Fisher and W. Selke, *Phys. Rev. Lett.* **44**:1502 (1980).
6. J. Vannimenus, *Z. Phys. B* **43**:141 (1981).
7. S. Inawashiro and C. J. Thompson, *Phys. Lett. A.* (1983), to appear.
8. S. Inawashiro, C. J. Thompson, and G. Honda, *J. Stat. Phys.* **33**:419 (1983).
9. T. Morita, *Phys. Lett.* **94A**:232 (1983).
10. T. Horiguchi and T. Morita, *J. Phys. A: Math. Gen.* **16**:3611 (1983).
11. T. Horiguchi and T. Morita, *Physica A* (1983), to appear.
12. S. Aubry, *Solitons and Condensed Matter Physics*, A. R. Bishop and T. Schneider, eds. (Springer, New York, 1978), pp. 264–277.
13. P. Bak, *Rep. Prog. Phys.* **45**:587 (1983).
14. S. Aubry, *J. Phys. (Paris)* **44**:147 (1983).